Anal Bioanal Chem (2009) 393:487–501
DOI 10.1007/s00216-008-2514-x

REVIEW

Micro- and nanotechnology for viral detection

Xuanhong Cheng · Grace Chen · William R. Rodriguez

Received: 16 September 2008 / Revised: 31 October 2008 / Accepted: 4 November 2008 / Published online: 4 December 2008

Abstract Since the identification of viruses at the start of the 20th century, detecting their presence has presented great challenges. In the past two decades, there has been significant progress in viral detection methods for clinical diagnosis and environmental monitoring. The earliest advances were in molecular biology and imaging techniques. Advances in microfabrication and nanotechnology have now begun to play an important role in viral detection, and improving the detection limit, operational simplicity, and cost-effectiveness of viral diagnostics. Here we provide an overview of recent advances, focusing especially on advances in simple, device-based approaches for viral detection.

Keywords Viral diagnosis · Bio-MEMS · Nanotechnology

X. Cheng
5 E. Packer Ave, Whitaker Laboratory, Bioengineering, Materials and Engineering, Lehigh University, Bethlehem, PA 18015, USA
e-mail: xuc207@lehigh.edu

G. Chen
Harvard–MIT Health Science and Technology, Massachusetts General Hospital, 114 16th Street, Charlestown, MA 02119, USA
e-mail: gracec@mit.edu

W. R. Rodriguez (✉)
Partners AIDS Research Center, Massachusetts General Hospital, 149 13th Street, Charlestown, MA 02129, USA
e-mail: wrodriguez@partners.org

Abbreviations

ADV	Adenovirus
AFM	Atomic-force microscopy
BV	Baculovirus
BVDV	Bovine viral diarrhea virus
CB3	Coxsackievirus B3
CCID	Cell culture infective dose
CMV	Cytomegalovirus
CPV	Canine parvovirus virus
DEP	Dielectrophoresis
EBV	Epstein–Barr Virus
EIA	Enzyme-linked immunoassays
ELISA	Enzyme-linked immunosorbent assay
FCM	Flow cytometry
HBV	Hepatitis B virus
HCV	Hepatitis C virus
HEV	Hepatitis E virus
HAU	Hemagglutination unit
HIV	Human immunodeficiency virus
HSV	Herpes simplex virus
IFA	Immunofluorescence assays
MEMS	Micro-electromechanical systems
MRI	Magnetic resonance imaging
PCR	Polymerase chain reaction
QD	Quantum dots
QCM	Quartz-crystal microbalance
PFU	Plaque-forming unit
RSV	Respiratory syncytial virus
SARS	Severe acute respiratory syndrome
SGIV	Singapore grouper iridovirus
SPR	Surface-plasmon resonance
$TCID_{50}$	50% tissue culture infective dose
TMV	Tobacco mosaic viruses
WSSV	White spot syndrome virus

Introduction

Why detect viruses?

Viruses are ubiquitous in human environments. They cause diseases in humans and in animals. They can contaminate supplies of water, food, and products intended to be sterile, for example biopharmaceuticals. Several viruses have changed the course of civilizations, including smallpox, yellow fever, polio, and most recently, HIV [6]. According to the Disease Control Priorities Project, three viruses—HIV, measles, and rotavirus— are among the top 10 leading contributors to the global burden of disease [7]. Two of the six CDC category A bioterror pathogens are viruses. Effective detection of viruses thus plays a critical role in medicine and public health, in bioindustry, and in biodefense.

All viruses share certain characteristics. Lacking most of the biological machinery to replicate, viruses are obligate intracellular entities. Each virus species consist of a unique set of genetic material, coding for as few as two (hepatitis D virus) or as many as 900 proteins (mimivirus) [8]. Structural viral proteins typically form a "capsid" shell that surrounds the nucleic acids and other proteins and gives the virus its shape. Capsids may or may not be further covered by a double-layer membrane, or envelope, derived from the host cell; the membrane may itself incorporate host proteins. Complete viral particles range in physical size from as small as 20 nm to as large as 400 nm in diameter.

History of viral detection

Although viral illnesses, especially smallpox and yellow fever, have been known since antiquity, the nature of viral illness remained mysterious until the late 19th century. In 1876, Alfred Mayer, a German agronomist, transmitted tobacco mosaic virus from one plant to another, fulfilling the Henle–Koch postulates for infectious agents [9]. In the 1880s, Louis Pasteur extracted rabies virus from the spinal cords of rabid dogs, and developed the rabies vaccine. The first detection of viruses may have been by the Scot John Buist in 1886, who stained scrapings of smallpox lesions and saw "elementary bodies" under the light microscope, which he mistook for bacteria; at a diameter of ~200 nanometers (nm), the largest smallpox viruses are at the limits of detection of light microscopy. Over the next 40 years, studies of the passage of "filterable agents"—small enough to squeeze through sub-micron porous filters—confirmed the infectious nature of these so-called "viruses" and established their role in diseases ranging from polio and yellow fever in humans to foot-and-mouth disease in cattle to tobacco mosaic disease in plants.

By the 1930s, physical chemistry studies of tobacco mosaic virus revealed that viruses contained protein and nucleic acid. Tobacco mosaic virus particles could be identified by sedimentation and x-ray crystallography, and were revealed to be elongated, 15×280 nm rods [10]. The first definitive visualization of individual viruses was by the German physician Helmut Ruska in 1940—fortuitously, his brother had invented the electron microscope [11, 12]. In the more than 60 years since then, viral detection has progressed rapidly; more than 1,500 human and animal viruses have now been identified.

Challenges to viral detection

Because of their small size, simple biology, and obligate intracellular life cycle, viruses present significant detection challenges. Since the 1940s, there have been three general approaches to detect viruses:

- analysis of the host organism's response to the virus, especially antibody serology;
- detection of a virus's molecular fingerprints, including viral proteins and viral nucleic acids; and
- direct sensing of whole viral particles.

Continuous technical improvements in each method have improved their speed, detection limit, accuracy, and cost-effectiveness. In this paper, we will provide a brief review on how recent advances in micro and nanotechnology affect viral detection, focusing especially on simple, device-based approaches. The methods reviewed are summarized in Table 1.

Serology: virus detection by anti-viral antibody

Given the challenge of detecting something as small as a virus, one successful strategy has been to look instead for changes an infectious virus induces in its host. Most viruses trigger mammalian immune systems to produce virus-specific antibodies, and antibody serology has become a straightforward and mature technology used primarily for diagnosing retrospective bacterial or viral infection. Because of a "window period" that encompasses the first few weeks after exposure (before the host immune response has generated virus-specific antibodies to viral antigens), serology is inaccurate for acute viral infections. Serology is also challenged to distinguish recent from remote infection, as, once generated, IgG antibodies, which are the easiest to detect, persist for life. This can be overcome to some extent by looking for the IgM subclass of antibodies, which appear early after a viral infection, and disappear over time.

Serologic tests for the presence of antibodies commonly use both surface-bound antibody–antigen binding reactions, including immunofluorescence assays (IFA), enzyme-linked immunoassays (EIA), and Western blotting [13,

Table 1 Summary of the methods reviewed in the paper

Method summary	Species detected	Detection limit	Sample volume	Steps to results	Accuracy	Time	Ref.
Antibody serology							
Colorimetric lateral diffusion immunochromatography	Antibody against HIV	sub pmol L^{-1} range	Fingerprick blood	0–1 step of centrifugation + sample loading	Screening test only	3–30 min	[18]
Amperometric sensing of enzyme-linked immunosorbent assay	Antibody against west Nile IgG	~1 pmol L^{-1} (1:10^7 antibody titer)	20 μL	>10 steps of reagent loading and rinsing	na	~2 h	[22]
Piezoelectric (QCM) antibody detection	Antibody against African swine fever virus or M13 phage	A few nmol L^{-1}	100–200 μL	Sample loading and rinsing	na	30 min	[23, 24]
Colorimetric lateral diffusion immunochromatography	Influenza A and B antigen	10^2–10^4 free particles mL^{-1}	100 μL–3 mL	0–2 steps of protein extraction + sample loading	Sen.[a] ~33–100%Spec.[b] ~ 95–100%	15–30 min	[27, 96]
Viral molecular markers—viral antigen							
Sandwich assay on magnetic beads, detection by chemiluminescence	HCV Core protein	Viral concentration equivalent to 100,000 RNA copies mL^{-1}	A few hundred microliters	Automated analyzer (Abott Architect)	Sen.[a] >97% Spec.[b] >99%	200 assays per hour	[25]
Sandwich assay on nanoarray and detection by AFM	HIV-1 antigen p24	25 fg p24 mL^{-1} (single fmol L^{-1})	1 μL	>5 steps of sample purification and immuno-binding	na	6 h	[28]
Viral molecular markers—nucleic acid							
Sample preparation for PCR							
Microchips for viral particle separation and RNA extraction	Orchid virus RNA	2000 copies mL^{-1}	100–200 μL	Single sample loading to yield PCR template + off-chip PCR and detection	na	2–3 h total	[1, 34, 37]
Paramagnetic beads for viral particle enrichment and laser irradiation for viral lysis	HBV DNA and yellow fever RNA	1,000–10,000 pfu mL^{-1}	100 μL	0–6 steps to yield viral genome + off-chip PCR and detection	na	12–15 min genome extraction	[35, 36]
Paramagnetic particle for viral RNA enrichment	HCV RNA	33 copies of RNA mL^{-1}	300 μL	>5 steps to yield viral RNA + off-chip PCR and detection	Sen.[a] 93%; Spec.[b] 100%	20 Min genome extraction	[38]
Nano-probe array for viral capture and lysis	Vaccinia DNA	9×10^9 pfu mL^{-1}	100 μL	1 step to yield viral genome + off-chip PCR and detection	na	<60 min viral capture and DNA extraction	
PCR chip							
PCR and capillary electrophoresis chip, fluorescence detection on chip	SARS-coronavirus RNA	~100 copies cDNA mL^{-1}	A few microliters	>10 steps to prepare viral cDNA	Sens.[a] 94% Spec.[b] na	50–60 min on chip	[47]

Table 1 (continued)

Method summary	Species detected	Detection limit	Sample volume	Steps to results	Accuracy	Time	Ref.
PCR product detection							
Lateral diffusion immunochromatography and fluorescence detection	Papillomavirus type 16 DNA	15 pmol L^{-1} amplicon	2 μL amplicon	Conventional PCR + 2–3 mixing steps after PCR	Prescreening: Sen.[a] 83% Spec[b] 83% Confirmatory: Sen.[a] 100% Spec[b] 100%	Screening: 30–60 min after PCR Confirmatory: 1–2 h after PCR	[60]
Microarray for cDNA sandwich and detection by silver stain enhancement	HEV RNA	>100 fmol L^{-1} amplicon (1 particle mL^{-1} before amplification)	100 μL	Conventional PCR + >10 steps after PCR	na	20–30 min after PCR	[51]
Surface hybridization and electrochemical detection by stripping chronopotentiometry	HBV RNA	20 pmol L^{-1} amplicon	300 μL	Conventional PCR + >10 steps after PCR	na	40 min after PCR	[56]
Surface hybridization and detection by fluorescence de-quenching	Dengue virus RNA	~10 μmol L^{-1} amplicon	A few μL amplicon	Conventional PCR + Single step of sample loading after PCR	na	1 h after PCR	[61]
Hybridization on microbeads and detection using liposomes carrying fluorescent dyes	Dengue virus RNA	50 pmol L^{-1} amplicon	1 μL	Conventional PCR + 4 steps after PCR	Sen.[a] 100% Spec.[b] na	20–25 min after PCR	[53, 97]
Surface hybridization and electrical detection by enzyme coupled redox reaction	HSV, CMV EBV nucleic acid	2 nmol L^{-1} amplicon	10 μL per amplicon	Conventional PCR + >10 steps after PCR	na	~1 h after PCR	[55]
Automated microchip for hybridization and sequencing	Influenza A	375 fmol L^{-1} amplicon	100 μL amplicon	Conventional PCR + single sample loading	Comparable with manual hybridization, >90% accuracy	<2 h after PCR	[62]
Fully integrated lab on a chip devices							
Microchip for viral enrichment, lysis, amplification and detection	Dengue virus serotype 2 and enterovirus 71, bacteria (*Bacillus anthracis* and *Bordetella pertussis*)	100–10^6 pfu mL^{-1}	1–25 μL	Single step of sample loading	na	30 min–4 h	[64, 65]
Combinatorial molecular assays							
Fluorescent lateral diffusion for protein and amplicon simultaneous detection	Antibody against HIV, HIV antigen and RNA	na	300 μL	Single step of sample loading	na	Na	[67]
Protein sandwich assay on microelectrodes for simultaneous and electrical detection of 5 HBV indices by	HBV antibody and antigen	1 ng mL^{-1} antibody or antigen	0.25 mL min^{-1}	Single step of sample loading, continuous injection of reagents using a syringe pump	Comparable with ELISA	10 min	[66]

Whole particle viral detection							
Optical detection methods							
Dynamic light scattering	Virus-like particles	4.6 μg mL^{-1}	~500 μL	2–3 steps to purify virus + sample loading	na	10 min	[71]
Fluorescence microscopy	Dengue, Vaccinia	5 pmol L^{-1}	~5 μL	>10 steps to purify and label virus	na	~2 h	[72, 73]
Flow cytometry	BV, RSV, Influenza A, ADV	10^5–10^7 virions mL^{-1}	~100 μL	0 (scattering) to over 10 steps (fluorescent labeling) to purify and label virus	Correlation coefficient up to 0.999 between known viral concentrations and the measured slope	1–2 h	[74–76, 98]
Interferometry	HSV-1	850 mL^{-1}	A few microliters	Na	Correlation coefficient ~0.95 between known viral concentrations and the measured slope	~1 h	[4]
Micro/nanoparticles as imaging agents	RSV, SGIV, MS2 bacteriophage	10^5–10^9 mL^{-1}	<100 μL	1 to over 10 steps to purify and label virus	Spec.[b] up to 99% for model virus in buffer	1–3 h	[77–81]
Surface plasmon resonance	WSSV	2.5 ng mL^{-1}	100 μL	Single step of sample loading	na	30 min	[82]
Electro-mechanical detection methods							
Quartz-crystal microbalance	HSV1, TMV, orchid viruses	10^3–10^9 mL^{-1}	1 μL–mLs	0–5 steps to purify viruses	na	~40 min	[83–87]
Atomic-force microscopy	CPV, CB3	10^8 mL^{-1}	1 μL	>5 steps to purify and immobilize viruses	na	30 min	[99]
Microcantilevers	Vaccinia, BV	10^5–10^8 mL^{-1}	A few microliters	1–3 steps to purify and immobilize viruses	na	30–60 min	[88–90]
Electromagnetic detection methods							
Nanowire sensing	Influenza A, avian ADV and avian paramyxovirus	10^8 mL^{-1}	150 μL h^{-1}	0–3 steps to purify viruses	na	Minutes to 1 h depending on viral concentration	[92]
Conductometric sensing	BVDV	10^3 CCID mL^{-1}	100 μL	Single step of viral loading	na	10 min	[5]
Resistive pulse method	RMuLV, SSV, M-PMV, FeLV, RD-114, PBCV-1	10^7 mL^{-1}	>10 μL	Single step sensing, purification required	Within 15%	Minutes	[93, 94]
Magnetic relaxation detection	HSV, ADV	10^3 mL^{-1}	100 μL	Single step of mixing	na	~30 min	[3]

[a] Sensitivity (Sen.) refers the proportion of people with the disease who have a positive test result
[b] Specificity (Spec.) refers to the proportion of people without the disease who have a negative test result
na, not available

14], and solution-phase reactions, such as hemagglutination inhibition (HI), complement fixation (CF), particle agglutination [15], and plaque-reduction neutralization.

Solid-phase IFA and EIA are currently the most popular anti-viral antibody detection platforms. Both types of assay rely on creating a sandwich structure around the target antibody, bound specifically between a surface-immobilized capture antigen and a detection molecule (e.g., a secondary anti-Ig antibody, or protein A). In IFAs, the detection tag is a fluorescent dye, the surface accumulation of which is indicative of the target antibody presence and is observed under a fluorescence microscope, fluorimeter, or fluorescence scanner. IFAs involve two binding steps, are relatively simple to operate, but usually necessitate skilled laboratory workers and the availability of a fluorescence detector.

In contrast to IFAs, EIAs use an enzyme as the detection agent. After formation of the sandwich structure on a solid support and extensive rinsing of unbound enzymes, a chromogenic enzyme substrate is supplied. The reaction catalyzed by the enzyme results in a color change in solution or on a surface, indicative of the presence of target molecules, which are typically anti-viral antibodies [16, 17]. An EIA setup often employs a membrane strip or a 96-well microplate, and can have a detection limit down to the sub-picomolar range [18].

In the last few decades, rapid lateral diffusion immunochromatographic assay platforms requiring only a single handling step have become popular for point-of-care uses, and have made disease diagnosis possible in remote settings. In these assays (Fig. 1), a membrane strip serves as the solid support that carries a surface-immobilized antigen line or spot for target capture. The strip is also impregnated on one end with a loosely bound detection molecule conjugated with dyes or nanoparticles (such as colloidal gold). As a fluid sample is placed on the sample pad, the detection molecule binds to the target antibody in the sample, and the complex is carried forward to the antigen line/spot by capillary force. Binding of the target antibody to the antigen on the capture line then leads to a visible color change. These assays are rapid (~15 min) and easy to operate (single-step), require small amounts of blood or other biological samples (ca a few hundred microliters) and can be deployed in low-resource, field settings. As a result, commercial rapid-assay kits are available for detecting numerous viruses. For HIV diagnosis alone, there are at least six FDA-approved rapid antibody tests [18, 19] using whole blood, serum, plasma and/or oral fluid as the target sample, and more than 20 rapid HIV tests have been evaluated by the World Health Organization's pre-qualification program [20]. On the down side, lateral flow immunoassays are slightly less sensitive [14] and are only semi-quantitative. For example, a few lateral flow strip kits for acute dengue infection have been found to have sensitivity lower than 25% [21].

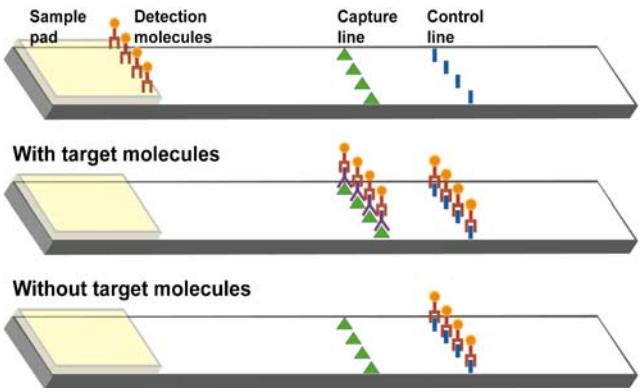

Fig. 1 Schematic diagram showing a lateral diffusion immunochromatographic strip and the working principle. In the presence of the target molecules, the detection agent will accumulate on both the capture and control lines, and change the color on the lines. Otherwise, only the control line will change color

From the MEMS device perspective, a few viral antibody detection bio-chips have been constructed to improve the detection limit and diagnostic sensitivity of EIAs, including amperometric [22] and piezoelectric [23] immunosensors. The detection agent in the amperometric immunosensor is an enzyme that catalyzes electron production. The sensor requires multiple rinsing and incubation steps to form a sandwich structure and to accomplish the electrochemical reaction. In contrast, piezoelectric sensors detect the surface formation of antibody–antigen complexes directly, without the need for a detection molecule, thus requiring only a single sample-introduction step, followed by washing. Binding of the target antibody to the piezo material changes its intrinsic vibration frequency, which is measurable in real time. In one attempt to improve the detection limit of a piezoelectric sensor, Yang et al. [24] immobilized multilayers of viral particles on a quartz-crystal microbalance substrate. Using this approach, the authors were able to detect 7 nmol L^{-1} of antibody against the immobilized virions.

Although simple and sensitive, challenges in quantifying virions, detecting acute infection, distinguishing acute from remote viral infection, or monitoring disease progression limit the practical utility of serology for many applications in viral diagnosis. The use of intrinsic viral molecules—for example nucleic acid and proteins—reduces the pre-seroconversion window period and opens up the possibility of acute viral diagnosis and virus quantification.

Detection of viral molecular fingerprints

Viral antigen detection

Viral antigen detection assays share many of the characteristics of the assays used for antibody serology, and many of

them have adopted the formats described above, including the lateral flow, EIA, and IFA platforms. Other approaches used to detect viral antigens include electrochemiluminescence, Western blot, radioimmunoassay, and radioimmunobinding assay. Detailed descriptions and comparison of these assays can be found in a recent review by Peruski et al. [14].

Certain challenges arise in detecting viral antigens. For protein antigens, an additional step is generally required to extract the target protein from inside intact virions or host cells. If the host has developed an antibody response against the viral antigen, a treatment to disrupt the in vivo antigen–antibody complexes may also be necessary to release the viral antigen [25]. Similar to the serological tests, viral antigen detection on a solid support often suffers from unsatisfactory detection limits and low diagnostic sensitivity. For example, Weinberg et al. reported sensitivities between 40 and 80% for three commercially available influenza immunoassay kits based on EIA or rapid immunochromatographic lateral diffusion [26, 27].

Besides the conventional flat substrate platforms, for example 96-well microplates and lateral diffusion strips, viral antigen detection immunoassays have recently been carried out on microbeads. These beads promote antibody–antigen interaction in a solution phase, reducing the diffusion limitation often observed at a low analyte concentration. An example is illustrated by a magnetic microparticle-based sandwich assay for detection of HCV core protein antigen in blood [25]. In this fully automated platform reported by Leary et al., the target antigen is sandwiched between a capture antibody immobilized on magnetic beads and a detection antibody labeled chemiluminescently. The sandwich structure is purified and enriched by rinsing under a magnetic field. Diagnostic sensitivity and specificity are both >95%. The method also enables quantitation of the HCV core protein, which may indicate disease progression. Although the detection limit does not reach that of nucleic acid amplification, the simple, automated operation process may be an important advantage in some settings.

To improve the detection limit of an immunoassay, Lee et al. used atomic-force microscopy (AFM) to probe the immuno-sandwich structure comprising a surface-immobilized antibody, an HIV core protein antigen (p24), and a secondary antibody carrying gold nanoparticles [28]. Because of signal amplification by the nanoparticles and sensitive AFM measurement, this immunoassay can detect down to 25 fg mL^{-1} of target proteins in plasma, an improvement of two orders of magnitude over conventional ELISA.

Nucleic acid detection

Amplification of the viral genome sequence is, to date, the most sensitive approach for detection of viruses and

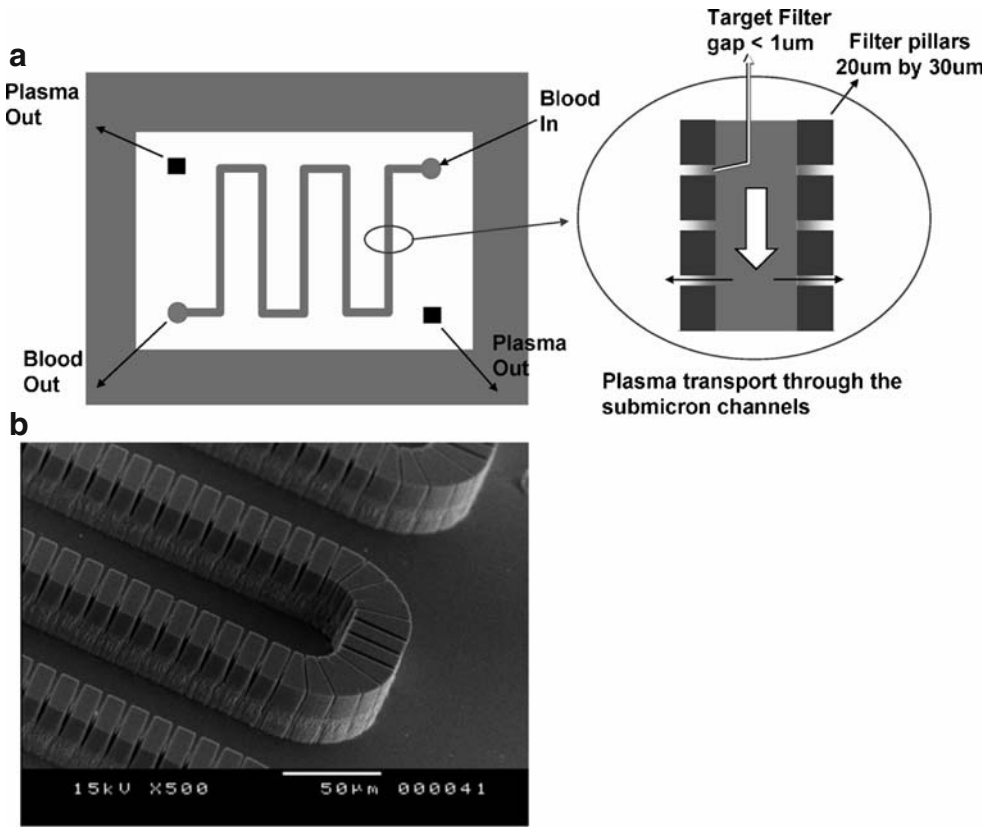

Fig. 2 (**a**) Schematic diagram of a shear-type filter for viral separation from whole blood. (**b**) SEM images of the filter [1]

differentiation of viral subtypes. Nucleic acid amplification has been considered the gold standard for diagnosis of many viral infections, and has been the subject of several recent reviews [29, 30]. Evolution of PCR and related nucleic acid amplification technologies has seen the widespread use of real-time, quantitative tests, which link amplification with detection, and enable quantification of the target sequence copy number [31–33]. Conventional nucleic acid amplification generally requires experienced personnel and well-equipped laboratory facilities, and the operating costs are high compared with serology and simpler methods. This is reflected in the price at US clinical laboratories: lateral flow immunoassays can often be done for $10 whereas PCR-based nucleic acid detection methods typically cost $100 for clinical assays. Recent technological advances have enabled automation and miniaturization of some of the steps involved—viral genome preparation, nucleic acid amplification, and amplicon detection. A complete, integrated system promises to make viral genetic analysis more widely affordable and available.

Viral genome preparation

For automated extraction of the viral genome from whole blood, Yobas et al. developed a microfluidic device comprising two components [1, 34]. The first component is a shear-type filter for viral separation (Fig. 2) fabricated by deep reactive-ion etching and SiO_2 deposition. In this filter chip, microposts with submicron spacing line a microfluidic channel that dynamically separates virus-rich plasma from blood cells. The second component of the device lyses virions and extracts and captures RNA on a silica surface for downstream PCR. RNA from ~2500 viral particles in each milliliter of blood can be reliably retrieved for a positive PCR result in this device. In a separate study, Cho et al. engineered a platform for preparation of HBV RNA from blood samples using affinity magnetic beads. Virions captured on the beads are separated from blood cells and plasma proteins, and then lysed by laser irradiation to release viral nucleic acids [35]. This CD device prepares a viral genome in 12 min with a single handling step, significantly reducing the sample-preparation time and handling process for PCR. In addition to immunoaffinity separation, anionic magnetic beads have also been constructed to enrich viruses based on non-specific interactions between virions and anionic polymers [36]. To reduce device fabrication cost, Bhattacharyya et al. recently developed thermal plastic chips impregnated with silica particles for solid-phase viral RNA extraction. This effort holds promise towards mass-produced disposable molecular diagnostic systems for infectious diseases. [37]

Magnetic beads are also widely used to enrich viral nucleic acid sequences. The magnetic beads are conjugated with a DNA strand to hybridize with a target sequence, and plasma components detrimental to the PCR reaction are efficiently separated from the beads by flushing the beads under a magnetic field. A few studies have demonstrated that magnetic particles can isolate down to tens of copies of target sequences from one milliliter of serum [38], which could then be amplified and detected by conventional means.

Electrical approaches have recently been directly applied to viral sample handling. Park et. al. constructed a microfluidic chip with nano-electrode arrays to capture vaccinia viruses. The same electrodes were then used to generate a high electrical field for viral lysis to yield viral DNA. Thus a single device fulfills both viral enrichment and genome-preparation purposes [39]. Microelectrodes have also been used to hydrolyze water and the associated hydroxide ion production disrupts lipid membranes and produces the target genome [40].

PCR microchips

Numerous microchip methods have been developed for the thermal cycling process of PCR, with many variations on both stationary and flow-through designs. Microchamber arrays for high-throughput PCR reactions have been constructed by several laboratories, with a requirement for only nanoliter to picoliter volumes of reagents [41, 42]. Many chips also incorporate capillaries for electrophoresis and detectors for fluorescence or UV absorbance measurement. Advances in PCR microchips have been extensively reviewed elsewhere [43–47], some with direct references to viral detection purposes [30, 33, 48]. The advantages of these PCR microchips include small sample volume, integrated amplification and detection, and shorter analysis time.

Amplicon detection

As an alternative to the conventional use of electrophoresis for amplicon detection, power-free sandwich assays are also frequently used in both flat substrate and microbead formats (Fig. 3). Similar to the protein sandwich assays, the target DNA is hybridized to both a surface-immobilized capture probe and a detection probe. With proper design of the DNA sequences, sandwich assays can detect viral subtypes [49]. Attempts have also been made to create capture probe arrays for multiplexed detection of multiple targets [50]. In addition to traditional fluorescent and enzymatic detection molecules, novel tags have been designed on the basis of recent advances in nanotechnology. For example, Liu et al. conjugated a detection DNA sequence with gold nanoparticles which can catalyze a silver stain enhancement reaction for dark silver particle

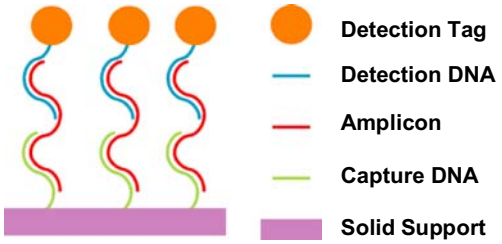

Fig. 3 Schematic diagram showing the molecular structure observed in a DNA sandwich assay. The solid support comes in either a flat surface or microbead form

deposition. As a result, the sandwich structure is visible to the naked eye on a solid substrate [51]. Another labeling agent recently popularized for biomolecule detection is the quantum dot (QD). Because of their size-dependent emission wavelength, QDs are useful for simultaneous detection of multiple targets for high-throughput viral analysis [52].

To improve the detection limit of sandwich assays, liposomes encapsulated with fluorescent or colorimetric molecules can be used to amplify the detection signal. A miniaturized set-up has been demonstrated in both microfluidic [53] and lateral diffusion strip formats using these liposomes [54]. The detection sensitivity is further improved by lysis of the surface-bound liposomes in a microfluidic device to de-quench the fluorophores in a concentrated state inside the liposomes.

The event of DNA hybridization can also be detected electrochemically using enzymes that catalyze redox reactions. Nebling et al. created a microelectrode array with patterned capture DNA sequences by use of this principle. Following a sandwich structure, electrical signal produced by alkaline phosphatase is detected in an addressable fashion on the array, enabling simultaneous analysis of multiple amplicons [55]. Alternatively, in a gold nanoparticle-catalyzed silver-deposition system, silver produced on the sandwich structure has been electrochemically oxidized to quantify the amount of captured target DNA [56].

Detection of amplicons, proteins, or whole-particle virions can also happen in a nanopore, into which the analyte entry results in an ion conduction change that can be detected electrically [57, 58]. Although early in its development, this resistive-pulse-sensing method can potentially be used for high-throughput DNA sequencing and mutation analysis, by labeling the nanopores with specific nucleic acids and studying the ion current patterns [59].

To simplify the amplicon detection procedure, rapid lateral diffusion strip chromatographic assays are implemented for both pre-screening and confirmatory purposes [60]. Analysis of PCR products on a nitrocellulose strip through lateral diffusion has been shown to detect down to 30 attomoles ($=10^{-18}$ mol) of genomic DNA from papillomavirus with 100% sensitivity and specificity using a viral culture sample. Another idea for simple DNA detection uses gold's property of quenching fluorophores in its close vicinity. In this approach, a fluorescently labeled DNA single strand is immobilized on gold for both capture and detection purposes. Fluorescence is only observed after hybridization with the target sequence, which distances the fluorophore from the gold surface. With a single mixing step, Li et al. demonstrated that this hybridization de-quenching approach can be used to detect PCR products of dengue virus in a microfluidic channel [61]. However, the detection limit is ~10 μmol L^{-1} because of a high background fluorescence signal.

Liu et al. at CombiMatrix recently developed an automated hybridization and sequencing chip for viral subtyping and genetic drift studies [62]. This integrated device contains a series of microfluidic controllers and uses a DNA microarray as the hybridization or sequencing substrate. It is attractive for its ability to detect multiple viruses and for the fully automated process.

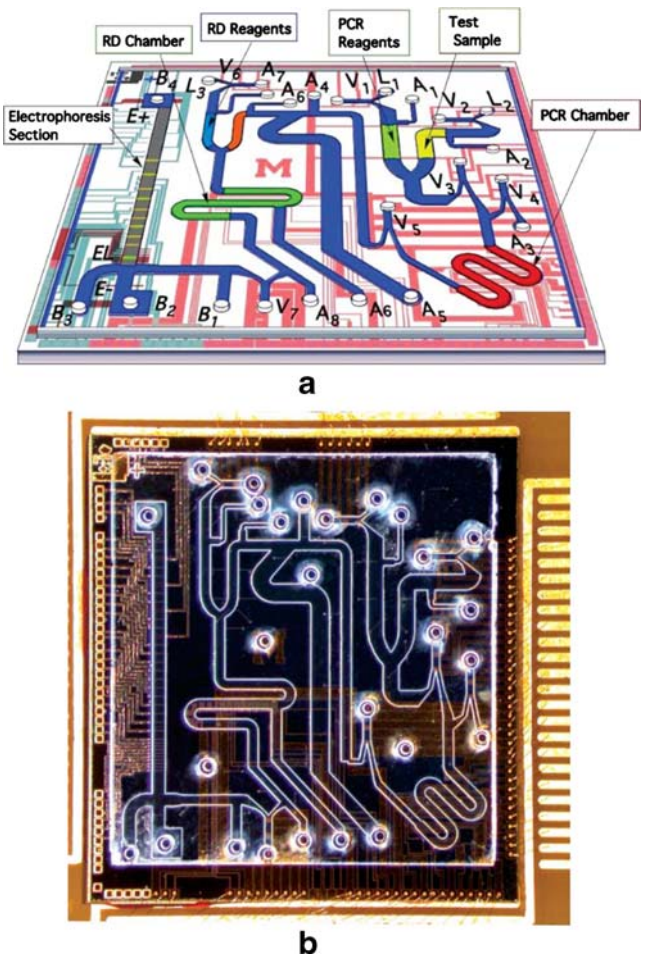

Fig. 4 Schematic diagram (**top**) and photograph (**bottom**) of a fully integrated lab-on-a-chip type device for viral genetic analysis developed by Pal et al. [2]

Fully integrated lab-on-a-chip devices

Recently, significant efforts have been made towards integrated genetic analysis microchips for sample-in, answer-out pathogen detection [2, 63, 64] (Fig. 4). These devices take in biological samples and perform, in a programmed fashion, the complete process of viral separation, lysis, nucleic acid amplification, and electrophoretic amplicon detection. Using such a device, Lien et al. detected dengue virus down to 10^2 pfu mL^{-1} within 4 h [65]. Another microchip by Easley et al. detects pathogens in blood in less than 30 min, though with compromised sensitivity [64].

Detection of multiple molecules

Detection of multiple types of viral molecule may be necessary in some cases to understand a patient's infection status or to confirm diagnosis. A few microdevice systems have been proposed or developed to achieve this goal. For example, Liang et al. [66] designed an integrated microfluidic device for simultaneous detection of multiple clinical markers used in HBV diagnosis. In this microchip, antibodies or antigens correlating to the five indices of HBV (HBsAb, HBcAb, HBeAb, HBsAg, and HBeAg) were immobilized on gold electrodes patterned inside a micro-device. The antibody–antigen interactions change the surface electrical property of the electrodes, which was detected amperometrically.

For confirmatory diagnosis in a single assay, Abrams [67, 68] proposed a microfluidic device of modular design for simultaneous identification of HIV antigens, antibodies, RNA, and DNA from an oral sample. The device employs four interrelated modules for sample acquisition, analyte extraction, amplification, detection, and signal analysis, respectively. All modules use similar fluid-control components and a common reporter, and all target molecules are detected in a lateral flow strip format.

Detection of intact viruses

The oldest methods for detecting the presence of viruses are based on identification of intact viruses. The plaque assay [69] and the hemagglutination assay [70] both served as the gold standard for viral detection for many decades before molecular analyses such as ELISA and PCR emerged. The viral concentration determined by these two tests, the plaque-forming unit (pfu) and the hemagglutination unit (HAU), are still widely used today. However, both the plaque assay and the hemagglutination assay are labor-intensive, difficult to calibrate, and are limited in their applicability to certain virus types. With the advent of molecular analyses, they now play a less important role in clinical viral diagnosis.

New methods are emerging that directly detect and enumerate intact viruses, on the basis of recent advances in optics, microfabrication, and nanotechnology. These methods have the potential to be more accurate in viral quantitation and less complex in sample preparation than molecular methods.

Optical detection methods

Dynamic light scattering

An early attempt at detecting viruses optically was made by Tsoka et al. in 1998, using dynamic light scattering to size virus-like particles (VLP) derived from yeast [71]. A commercial particle-size analyzer was used to study a population of VLPs with or without antibody attachment. It was found that the antibody-attached VLPs averaged 115 nm in diameter, significantly larger than the 77 nm average size without any antibody. The analysis process was completed in 10 min; the detection limit, 4.6 μg mL^{-1}, was low, however, and it is unclear whether the method will work with complex biological samples.

Fluorescence microscopy

Advances in fluorescence microscopy have enabled the direct observation of stained viruses both for studying viral behavior and as a possible diagnostic tool. Akin et al. trapped viruses by use of dielectrophoretic (DEP) filters, and observed the trapping process in real time by fluorescence microscopy [72]. Because of the requirement of de-ionized water as suspension medium and the non-specificity of DEP, the method is only applicable to highly purified viral samples. Zhang et al. fabricated an array of nanoscale fluidic chambers, each with a femtoliter volume, as an approach to compartmentalize dengue virus samples [73]. By labeling the viral particle and a specific antibody with two distinct fluorophores, and fluorescently probing each chamber for double-stained particles, they were able to determine the concentration of dengue viruses down to the nanomolar range, with potential improvement to a femtomolar detection limit in the future.

Flow cytometry

Flow cytometry (FCM) is widely used for the enumeration and subtyping of cells and other bio-particles in an aqueous solution. Several groups have recently developed FCM-based methods for quantification of viruses. Shen et al. [74] used a highly fluorescent nucleic acid dye, SYBR Green 1, to stain the DNA of baculovirus after fixation and membrane permeabilization. A commercial flow cytometer was then used to count the number of viral particles in the

sample. Steen [75] developed a custom-designed FCM with enhanced light scattering, which enabled direct detection of scatter from nanoparticles and viruses down to 70 nm in diameter. Ferris et al. [76] built a custom FCM instrument—named the single nanometric particle enumerator (SnaPE)—with a 0.5 μm probe size and femtoliter probe volume. The detection limit of this instrument was found to be 10^6 particles mL^{-1} using three different respiratory viruses. Stoffel et al. used a two-color, dual-staining method targeting both viral DNA and a capsid protein to enable measurement of unpurified viral samples, also using a custom designed FCM. As the data acquisition rate for FCM is in the kilohertz range, target particles are counted in a high-throughput fashion. However, sample preparation and staining are often required prior to FCM analysis, making the total assay a ~2-h process.

Micro/nanoparticles as imaging agents

Instead of staining the viruses directly by use of fluorescent dyes, micro/nanoparticles carrying detection tags and capable of recognizing the target virions are also used as labeling and imaging agents. These methods have the advantage of higher specificity towards the target virions, and improved imaging contrast compared with direct viral staining.

Agrawal et al. used two types of nanobead with different fluorescence colors to recognize viral particles at two binding sites [77, 78]. The particle and virus mixture was passed through a flow cytometer-based arrangement in which fluid at an aperture was excited at the two relevant wavelengths. The system could count co-localizations of the two colored particles as a viral passage event, thus enabling differentiation between virion-bound and unbound particles.

Bentzen [79] and Ang [80] both used highly fluorescent QDs as the imaging agents for detection of intact virions. Bentzen et al. used different colored QDs to co-localize nuclear and envelope proteins of the respiratory syncytial virus. Using a confocal fluorescent microscope to observe the stained virions, they were able to track in real time the progression of cell infection by viruses. Ang developed a microfluidic ELISA device that first trapped viral-recognizing microbeads in a filter structure, then captured virions on the beads, and, finally, detected the virions using fluorescent QDs conjugated with anti-viral antibodies. This device approach is faster, more sensitive, and better automated than the standard ELISA assay, but device fabrication requires high-resolution MEMS facilities.

Lee [81] developed a technique of force differentiation using magnetic beads in a uniform magnetic field to enumerate virions optically. An immuno-sandwich was first formed between a surface, the virions, and 1-μm magnetic beads. The magnetic field was then switched on perpendicular to the surface so that non-specific bonds attaching any beads to the surface would be broken, while the antibody-specific bonds holding together the immuno-sandwich structure remained attached. The surface was then imaged under a microscope, and the number of magnetic beads that remained attached was counted as the total number of viruses present in the original sample. Total assay time for this method was around one hour, and the detection limit was 10^5 particles mL^{-1}.

Interferometry

The principle of Young's interferometry was utilized by Ymeti et al. to produce a multiplexed, label-free viral particle detector with sensitivity in PBS down to 850 particles mL^{-1} [4] (Fig. 5). The device consists of a four-channel optical waveguide in which one channel is used as the reference while the others are functionalized to sense three different analytes. Monochromatic light from a laser is introduced at one end of the waveguide, and a CCD screen images the interference pattern formed at the opposite end. Binding of virus to a channel induces a phase change of the incident light, and the amount of phase shift is indicative of the viral concentration. Viral detection in serum was demonstrated with a suspension containing 10^5 particles mL^{-1}. The device could potentially be automated for use as a fast and portable point-of-care viral counter.

Surface plasmon resonance (SPR)

SPR is a label-free, optical technique for detection of refractive index change on a metal surface. In work by Lei et al. [82] antibody-immobilized gold nano-particles were adsorbed on a glass substrate as an SPR sensing surface, and binding of a shrimp virus was detected with a detection

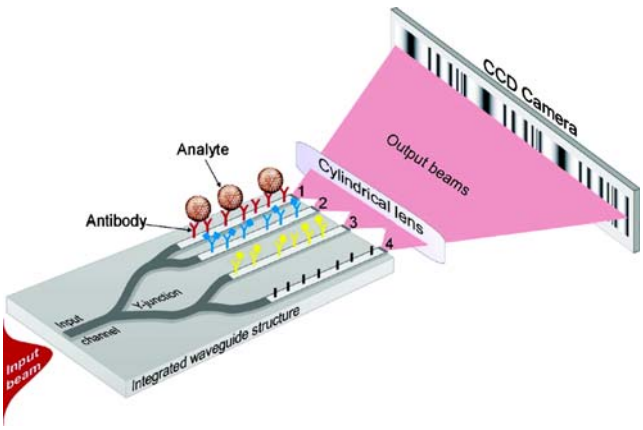

Fig. 5 Schematic diagram showing a Young's interferometer used for viral detection. *Channels 1, 2, and 3* indicate the measurement channels; *4* is the reference channel [4]

limit of 2.5 nanogram of virions per milliliter, which is an improvement of more than one order of magnitude compared with conventional ELISA. As a single sample-introduction step is involved in the whole detection process, the technique is a good candidate for point-of-care applications.

Electromechanical methods

Quartz-crystal microbalance (QCM)-based detection

The QCM is an established, commercially available mass sensor commonly used for quantitative measurement of the thickness of thin films. For the purpose of bio-detection, the surface of a quartz-crystal microchip is usually coated with antibodies against the target bio-molecules. The resonant frequency of the chip is measured before and after sample introduction, and binding of the target agents will result in an increase in mass that lowers the chip resonant frequency. Eun et al. used QCM in this mode of operation to detect orchid viruses from plant sap [83] and found a detection limit of approximately 1 ng virus per 5 μL sample, which is equivalent to around 10^7–10^8 viral particles per milliliter.

Hayden et al. used a QCM for detection of tobacco mosaic virus [84, 85]. Instead of using antibodies as the capture molecule, they used artificial receptors based on a molecularly imprinted polymer (MIPS) technique. Such polymer receptors have greater stability and thus much longer shelf-life than traditional antibody-functionalized QCM chips. However, the detection limit of this approach was not reported.

Cooper et al. found a novel mode of operation for QCM in a technique called rupture event scanning [86, 87]. They bound virus to the QCM chip using antibodies as usual, but instead of taking a mass measurement directly, they continued to increase the voltage until the vibrational energy ruptured the bonds holding the virus to the chip. They found that this technique enabled much more sensitive detection, and could resolve down to a single virion on a QCM chip. With a sample volume of 1 μL, this corresponded to a detection limit of 1000 particles mL^{-1}. They also showed that direct detection in serum was feasible.

Microcantilevers

Microcantilevers have been widely investigated for a number of biosensing applications. There are two common modes of operation, resonant mode and strain mode, both of which have been applied to viral detection. Gupta [88] and Ilic [89] both used the resonant mode to detect viral binding by sensing a change in the cantilever mass. Gupta used vaccinia samples at 10^9 particles mL^{-1}, and Ilic was able to detect baculovirus at 10^5 particles mL^{-1}. However, because of the dramatically reduced performance of resonating cantilevers in liquid, both methods require drying prior to mass measurement in air or vacuum.

Gunter et al. used piezoresistive cantilevers in the strain mode for viral sensing. Particle binding on these cantilevers induces a strain and changes their electrical resistance [90]. Such cantilevers have much simpler measurement circuitry and readout than the resonant cantilevers, but the detection limit is not as low. Gunter detected viral samples both in liquid and in aerosol form, at a concentration of approximately 10 μg mL^{-1}.

Electrical conductance methods

Nanowire detection

With advances in nanofabrication, a new class of nanowire field-effect transistors has been explored for biodetection [91]. Nanowires can be functionalized against the virus of interest, and binding of a charged viral particle produces a depletion or gain of charge in the nanowires, which can be measured as a simple conductance change. Using such a device, Patolsky et al. was able to detect binding and breaking-off events occurring between a single influenza A virion and a nanowire sensor [92].

Conductometric sensor

Another technique based on electrical conductivity measurement was developed by Muhammad-Tahir et al. to detect bovine viral diarrhea virus (BVDV) [5] (Fig. 6). This method uses a lateral flow approach to form conjugates between the target virus and a polyaniline-labeled antibody on a disposable membrane. This conjugate is then detected using the conducting property of polyaniline. The complete set up, including materials and readout electronics, is extremely simple and the detection limit was found to be 1000 cell culture infectious doses (CCID) mL^{-1}. However,

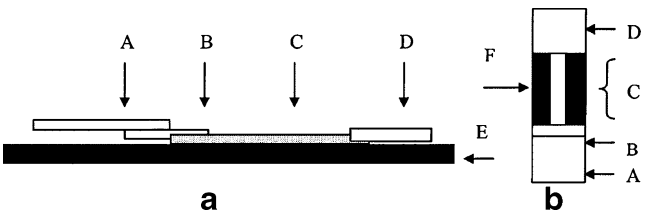

Fig. 6 Schematic diagram of the conductometric immunosensor created by Muhammad-Tahir et al. (**a**) Cross section view and (**b**) top view of the sensor. The sections are: (*A*) sample-application membrane, (*B*) conjugate membrane for polyaniline-labeled antibody, (*C*) capture membrane coated with (*F*) silver electrodes on both sides, (*D*) absorption membrane, and (*E*) copper wafer platform [5]

the sensing accuracy is relatively poor, making it only suitable as a screening diagnostic.

Resistive pulse technique

Detection of particles by monitoring the electrical resistance change as they pass through a narrow orifice is best known in the form of the Coulter counter. The technique makes use of the principle that biological particles are non-conducting at low frequencies, because of their membrane capacitance. When non-conducting particles displace a volume of conducting electrolyte (usually a salt buffer) inside the orifice, they momentarily increase the resistance measured across the orifice. The size of the resistance change is directly related to the volume of the particle. Coulter first described this method in the 1950s and commercially available instruments are widely used for enumeration and sizing of cells and other micrometer-sized particles. In the 1970s, Deblois and Wesley [93] described the use of a 400 nm diameter pore to accurately size a number of different viruses. The accuracy of the count and the sensitivity of detection was compromised by particle contaminants in the sample, and their lowest reliable sensitivity was 10^7 mL^{-1}. Their instrument, the "Nanopar", was capable of counting 10^9–10^{11} particles mL^{-1} in several minutes. More recently, Uram et al. was able to use a similar technique to detect the subtle size difference between plain and antibody-bound viruses [94]. The simplicity, speed, and low cost of this technique is highly attractive provided effective purification steps can be undertaken to isolate pure viral populations from the original sample.

Other methods

Atomic-force microscopy (AFM)

AFM is a useful study tool for imaging of viruses [95]. Recently, Nettikadan et al. developed a multiplexed sensing chip that uses AFM as the final detection step in a rapid viral diagnostic application. Miniature antibody capture domains were patterned using "ink-jet" protein array technology, and specific capture of three different viruses was shown to take place simultaneously without cross interference. The sample chip was cleaned and dried before AFM sensing, with the entire process taking around 30 min. The detection limit of this AFM approach was found to be 10^8 pfu mL^{-1}. Although the multiplexing capability of this technique is attractive, the cumber and expense of AFM limits the range of applications possible.

Magnetic relaxation detection

Magnetic nanoparticles can induce changes in the T2 relaxation time of surrounding water molecules and are often used as contrast agents for magnetic resonance imaging (MRI). An even more interesting property of these particles is that when they assemble into closely packed aggregates, the change they induce in the T2 time is significantly greater than the sum effect of the individual free particles. Perez et al. took advantage of this phenomenon for highly sensitive detection of viral particles by employing individual viruses as nucleation points for the assembly of iron oxide nanoparticles [3] (Fig. 7). The particles were functionalized against the virus of interest, and simple mixing with the target virions would lead to formation of magnetic aggregates. A tabletop relaxometer was then used to take T2 measurements, and it was found that the relaxation time increased with the viral concentration, making viral quantitation possible. The detection limit of this method is around 10^3 particles mL^{-1} and it can be further improved by increasing the magnetic field. As the measurement can be taken with both buffer and serum samples, this approach is plausible for robust and versatile clinical analyses.

Conclusion

In summary, technical breakthroughs have been reported in viral detection on both molecular and whole-particle levels. Many of these breakthroughs have taken advantage of recent advances in the rapidly growing micro and nanotechnology to bring improvements to the speed, sensitivity,

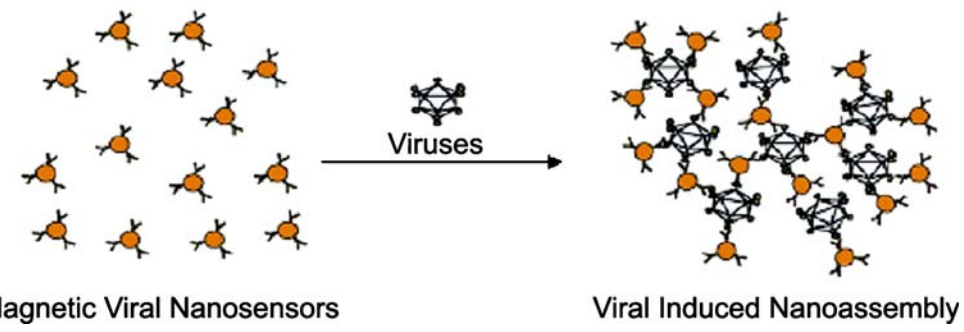

Fig. 7 Diagram of viral-induced nanoassembly of magnetic nanoparticles. The viral-induced nanoassembly is detectable by magnetic resonance imaging [3]

operability, and portability of viral diagnostics. Further efforts in device integration, process automation, cost reduction, and improved accuracy will re-shape future viral diagnosis for access at point-of-care and even home settings.

References

1. Yobas L, Ji HM, Hui WC, Chen Y, Lim TM, Heng CK, Kwong DL (2007) IEEE J Solid-State Circuit 42:1803–1813
2. Pal R, Yang M, Lin R, Johnson BN, Srivastava N, Razzacki SZ, Chomistek KJ, Heldsinger DC, Haque RM, Ugaz VM, Thwar PK, Chen Z, Alfano K, Yim MB, Krishnan M, Fuller AO, Larson RG, Burke DT, Burns MA (2005) Lab Chip 5:1024–1032
3. Perez JM, Simeone FJ, Saeki Y, Josephson L, Weissleder R (2003) J Am Chem Soc 125:10192–10193
4. Ymeti A, Greve J, Lambeck PV, Wink T, van Hovell S, Beumer TAM, Wijn RR, Heideman RG, Subramaniam V, Kanger JS (2007) Nano Lett 7:394–397
5. Muhammad-Tahir Z, Alocilja EC, Grooms DL (2005) IEEE Sens J 5:757–762
6. Oldstone MBA (1998) Viruses, plagues, and history. Oxford University Press
7. Mathers CD, Lopez AD, Murray CJL (2006) In: Global burden of disease and risk factors. Oxford University Press, New York, pp 45–93
8. Mrazek J, Karlin S (2007) Proc Natl Acad Sci USA 104:5127–5132
9. Crawford D (1998) The invisible enemy: a natural history of viruses. Oxford University Press
10. Wendell S In Nobel Lecture, December 12, 1946
11. Ruska H, Borries BV, Ruska E (1939) Arch Virol 1:15
12. Kruger DH, Schneck P, Gelderblom HR (2000) Lancet 355:1713–1717
13. Koivunen ME, Krogsrud RL (2006) Labmedicine 37:8
14. Peruski AH, Peruski LF (2003) Clin Diagn Lab Immunol 10:506–513
15. Yamaguchi K, Yonemura Y, Okabe H, Takahama Y, Nagai S, Yamaguchi H, Hira K (2003) Clin Chem 49:275–280
16. Granade TC, Phillips SK, Parekh B, Gomez F, Kitson-Piggott W, Oleander H, Mahabir B, Charles W, Lee-Thomas S (1998) Clin Diagn Lab Immunol 5:171–175
17. Wu SJL, Hanson B, Paxton H, Nisalak A, Vaughn DW, Rossi C, Henchal EA, Porter ER, Watts DM, Hayes CG (1997) Clin Diagn Lab Immunol 4:452–457
18. Greenwald JL, Burstein GR, Pincus J, Branson B (2006) Curr Infect Dis Rep 8:125–131
19. http://www.cdc.gov/hiv/topics/testing/rapid/rt-comparison.htm, last accessed: February 4, 2008
20. http://www.who.int/diagnostics_laboratory/evaluations/hiv/en/, last accessed: August 13, 2008
21. Cohen AL, Dowell SF, Nisalak A, Mammen PM, Petkanchanapong W, Fisk TL (2007) Trop Med Int Health 12:47–51
22. Ionescu RE, Cosnier S, Herrmann S, Marks RS (2007) Anal Chem 79:8662–8668
23. Uttenthaler E, Kosslinger C, Drost S (1998) Biosens Bioelectron 13:1279–1286
24. Yang LMC, Diaz JE, McIntire TM, Weiss GA, Penner RM (2008) Anal Chem 80:933–943
25. Leary TP, Gutierrez RA, Muerhoff AS, Birkenmeyer LG, Desai SM, Dawson GJ (2006) J Med Virol 78:1436–1440
26. Allwinn R, Preiser W, Rabenau H, Buxbaum S, Sturmer M, Doerr HW (2002) Med Microbiol Immunol 191:157–160
27. Weinberg A, Walker ML (2005) Clin Diagn Lab Immunol 12:367–370
28. Lee KB, Kim EY, Mirkin CA, Wolinsky SM (2004) Nano Lett 4:1869–1872
29. Espy MJ, Uhl JR, Sloan LM, Buckwalter SP, Jones MF, Vetter EA, Yao JDC, Wengenack NL, Rosenblatt JE, Cockerill FR, Smith TF (2006) Clin Microbiol Rev 19:165–256
30. Yang S, Rothman RE (2004) Lancet Infect Dis 4:337–348
31. Bustin SA (2002) J Mol Endocrinol 29:17
32. Ginzinger DG (2002) Exp Hematol 30:503–512
33. Mackay IM, Arden KE, Nitsche A (2002) Nucleic Acids Res 30:1292–1305
34. Hui WC, Yobas L, Samper VD, Heng CK, Liw S, Ji HM, Chen Y, Cong L, Li J, Lim TM (2007) Sens Actuators A 133:335–339
35. Cho YK, Lee JG, Park JM, Lee BS, Lee Y, Ko C (2007) Lab Chip 7:565–573
36. Veyret R, Elaissari A, Marianneau P, Sall AA, Delair T (2005) Anal Biochem 346:59–68
37. Bhattacharyya A, Klapperich CA (2008) Sens Actuators B 129:693–698
38. Miyachi H, Masukawa A, Ohshima T, Hirose T, Impraim C, Ando Y (2000) J Clin Microbiol 38:18–21
39. Park K, Akin D, Bashir R (2007) Biomed Microdevices 9:877–883
40. Di Carlo D, Ionescu-Zanetti C, Zhang Y, Hung P, Lee LP (2005) Lab Chip 5:171–178
41. Marcus JS, Anderson WF, Quake SR (2006) Anal Chem 78:956–958
42. Nagai H, Murakami Y, Morita Y, Yokoyama K, Tamiya E (2001) Anal Chem 73:1043–1047
43. Sanders GHW, Manz A (2000) Trends Anal Chem 19:364–378
44. Zhang CS, Xu JL, Ma WL, Zheng WL (2006) Biotechnol Adv 24:243–284
45. Kaltenboeck B, Wang CM (2005) In: Advances in clinical chemistry. vol Elsevier Academic Press, San Diego, pp 219–259
46. Jakeway SC, de Mello AJ, Russell EL (2000) Fresenius J Anal Chem 366:525–539
47. Zhou ZM, Liu DY, Zhong RT, Dai ZP, Wu DP, Wang H, Du YG, Xia ZN, Zhang LP, Mei XD, Lin BC (2004) Electrophoresis 25:3032–3039
48. Chan AB, Fox JD (1999) Rev Med Microbiol 10:185–196
49. Gonzalez R, Masquelier B, Fleury H, Lacroix B, Troesch A, Vernet G, Telles JN (2004) J Clin Microbiol 42:2907–2912
50. Yeung SW, Lee TMH, Cai H, Hsing IM (2006) Nucleic Acids Res 34:7
51. Liu HH, Cao X, Yang Y, Liu MG, Wang YF (2006) J Biochem Mol Biol 39:247–252
52. Gerion D, Chen FQ, Kannan B, Fu AH, Parak WJ, Chen DJ, Majumdar A, Alivisatos AP (2003) Anal Chem 75:4766–4772
53. Zaytseva NV, Montagna RA, Baeumner AJ (2005) Anal Chem 77:7520–7527
54. Baeumner AJ, Schlesinger NA, Slutzki NS, Romano J, Lee EM, Montagna RA (2002) Anal Chem 74:1442–1448
55. Nebling E, Grunwald T, Albers J, Schafer P, Hintsche R (2004) Anal Chem 76:689–696
56. Hanne H, Ghourchian H, Ziaee AA (2007) Anal Biochem 370:195–200
57. Harrell CC, Choi Y, Horne LP, Baker LA, Siwy ZS, Martin CR (2006) Langmuir 22:10837–10843
58. Bayley H, Martin CR (2000) Chem Rev 100:2575–2594
59. Iqbal SM, Akin D, Bashir R (2007) Nat Nanotechnol 2:243–248
60. Corstjens P, Zuiderwijk M, Brink A, Li S, Feindt H, Neidbala RS, Tanke H (2001) Clin Chem 47:1885–1893
61. Li YT, Liu HS, Lin HP, Chen SH (2005) Electrophoresis 26:4743–4750

62. Liu RH, Lodes MJ, Nguyen T, Siuda T, Slota M, Fuji HS, McShea A (2006) Anal Chem 78:4184–4193
63. Waters LC, Jacobson SC, Kroutchinina N, Khandurina J, Foote RS, Ramsey JM (1998) Anal Chem 70:158–162
64. Easley CJ, Karlinsey JM, Bienvenue JM, Legendre LA, Roper MG, Feldman SH, Hughes MA, Hewlett EL, Merkel TJ, Ferrance JP, Landers JP (2006) Proc Natl Acad Sci USA 103:19272–19277
65. Lien KY, Lin JL, Liu CY, Lei HY, Lee GB (2007) Lab Chip 7:868–875
66. Liang KZ, Mu WJ, Huang MY, Yu ZX, Lai QK (2007) Biomed Microdevices 9:325–333
67. Abrams WR, Barber CA, McCann K, Tong G, Chen ZY, Mauk MG, Wang J, Volkov A, Bourdelle P, Corstjensd P, Zuiderwijk M, Kardos K, Li S, Tanke HJ, Niedbala RS, Malamud D, Bau H (2007) In: Oral-based diagnostics, vol 10. Blackwell, Oxford, pp 375–388
68. Chen ZY, Mauk MG, Wang J, Abrams WR, Corstjens P, Niedbala RS, Malamud D, Bau HH (2007) In: Oral-based diagnostics, vol 10. Blackwell, Oxford, pp 429–436
69. Russell WC (1962) Nature 195:2
70. Donald HB, Isaacs A (1954) J Gen Microbiol 10:8
71. Tsoka S, Holwill I, Hoare M (1999) Biotechnol Bioeng 63:290–297
72. Akin D, Li HB, Bashir R (2004) Nano Lett 4:257–259
73. Zhang YX, Bahns JT, Jin QL, Divan R, Chen LH (2006) Anal Biochem 356:161–170
74. Shen CF, Meghrous J, Kamen A (2002) J Virol Methods 105:321–330
75. Steen HB (2004) Cytom A 57A:94–99
76. Ferris MM, McCabe MO, Doan LG, Rowlen KL (2002) Anal Chem 74:1849–1856
77. Agrawal A, Tripp RA, Anderson LJ, Nie SM (2005) J Virol 79:8625–8628
78. Agrawal A, Zhang CY, Byassee T, Tripp RA, Nie SM (2006) Anal Chem 78:1061–1070
79. Bentzen EL, House F, Utley TJ, Crowe JE, Wright DW (2005) Nano Lett 5:591–595
80. Liu WT, Zhu L, Qin QW, Zhang Q, Feng HH, Ang S (2005) Lab Chip 5:1327–1330
81. Lee GU, Metzger S, Natesan M, Yanavich C, Dufrene YF (2000) Anal Biochem 287:261–271
82. Lei Y, Chen HY, Dai HP, Zeng ZR, Lin Y, Zhou FM, Pang DW (2008) Biosens Bioelectron 23:1200–1207
83. Eun AJC, Huang LQ, Chew FT, Li SFY, Wong SM (2002) J Virol Methods 99:71–79
84. Hayden O, Bindeus R, Haderspock C, Mann KJ, Wirl B, Dickert FL (2003) Sens Actuators B 91:316–319
85. Dickert FL, Hayden O, Bindeus R, Mann KJ, Blaas D, Waigmann E (2004) Anal Bioanal Chem 378:1929–1934
86. Cooper MA (2003) Meas Sci Technol 14:1888–1893
87. Cooper MA, Dultsev FN, Minson T, Ostanin VP, Abell C, Klenerman D (2001) Nat Biotechnol 19:833–837
88. Gupta A, Akin D, Bashir R (2004) Appl Phys Lett 84:1976–1978
89. Ilic B, Yang Y, Craighead HG (2004) Appl Phys Lett 85:2604–2606
90. Gunter RL, Delinger WG, Manygoats K, Kooser A, Porter TL (2003) Sens Actuators A 107:219–224
91. Li Y, Qian F, Xiang J, Lieber CM (2006) Mater Today 9:18–27
92. Patolsky F, Zheng GF, Hayden O, Lakadamyali M, Zhuang XW, Lieber CM (2004) Proc Natl Acad Sci USA 101:14017–14022
93. Deblois RW, Wesley RKA (1977) J Virol 23:227–233
94. Uram JD, Ke K, Hunt AJ, Mayer M (2006) Small 2:967–972
95. Kuznetsov YG, Malkin AJ, Lucas RW, Plomp M, McPherson A (2001) J Gen Virol 82:2025–2034
96. Mcfarland E, Yup A, Joshi S, Lovell S, Stahler J, Finnerty C, Pope B, Newman J, Crews V (2005) In: Clinical Virology Symposium
97. Zaytseva NV, Goral VN, Montagna RA, Baeumner AJ (2005) Lab Chip 5:805–811
98. Stoffel CL, Kathy RF, Rowlen KL (2005) Cytom A 65A:140–147
99. Nettikadan SR, Johnson JC, Mosher C, Henderson E (2003) Biochem Biophys Res Commun 311:540–545